Supplementary information: Atomically Thin Pt Shells on Au Nanoparticle Cores: Facile Synthesis and Efficient Synergetic Catalysis

C. Engelbrekt[a], N. Šešelj[a], R. Poreddy[b], A. Riisager[b], J. Ulstrup[a], J. Zhang[a]*

[a] *NanoChemistry, Department of Chemistry, Technical University of Denmark, Kemitorvet 207, 2800, Kgs. Lyngby, Denmark*
[b] *Centre for Catalysis and Sustainable Chemistry, Department of Chemistry, Technical University of Denmark, Kemitorvet 207, 2800, Kgs. Lyngby, Denmark*

Experimental details

Chemicals

All chemicals were used as received. Aqueous solutions were prepared from $HAuCl_4 \cdot 3H_2O$ (99.99%, Sigma-Aldrich) and $H_2PtCl_6 \cdot xH_2O$ (99.9+%, Sigma-Aldrich), D-(+)-Glucose (for laboratory use, Sigma), soluble Zulkowsky starch (pro analysi, Merck), 2-*(N*-morpholino)ethanesulfonic acid (MES) hydrate (99.5%, Sigma-Aldrich) for the synthesis of Au and Pt based nanostructures. pH of the MES stock solution was adjusted with KOH (99.99%, Sigma-Aldrich). 0.1 M H_2SO_4 solution was prepared from 96%, H_2SO_4 (Suprapur, Merck) for electrochemical measurements. Formic acid (98%, Fluka), methanol (≥99.8%, Sigma-Aldrich) and ethanol (≥99.9%, Merck) were used for electrooxidation experiments. Toluene (99.9%, Sigma-Aldrich), benzamide (99%, Aldrich), benzoic acid (99%, Aldrich), levulinic acid (≥98%, Aldrich), and methyl levulinate (≥98%, Aldrich) were used for hydrogenation reactions. Millipore water was used throughout the study for cleaning and preparation of solutions.

Characterization techniques

Ultraviolet-visible light (UV-Vis) extinction spectra were measured with a model 8453 spectrophotometer from Agilent Technologies (Santa Clara, USA), equipped with a 1 cm light path quarts cuvette.

Nanoparticle tracking analysis (NTA) was achieved with an LM10 from NanoSight (Wiltshire, UK) fitted with a red laser. Samples were diluted prior to measurement in Millipore water. After injection of the diluted sample into the laser block, the system was allowed to equilibrate for 30 s before recording to ensure reproducibility. The videos were processed with NTA 3.0 using automated settings.

Electrochemical measurements were carried out on a three-electrode system using an Autolab PGSTAT12 potentiostat from Metrohm (Netherlands). The electrochemical glass cell was home-made with three separate chambers for working electrode (WE), counter electrode (CE) and reference electrode (RE), respectively. Nanoparticles/catalyst loaded on basal plane graphite (BPG) (ø = 5 mm, Pine Instrument Company, Grove, USA) or glassy carbon (ø = 4 mm) were used as WEs. BPG and glassy carbon electrodes were freshly cleaned by mechanical polishing on SiC sand papers and 1.0, 0.3 and 0.1 µm Al_2O_3 slurry on a felt disk followed by ultrasonication twice in Millipore water. 10-30 µL nanoparticle solution was drop cast on the freshly polished electrodes and dried at 60 °C for 2 hours or room temperature (r.t.). >5 h. Electrodes for EC experiments with G-CB supported NPs were prepared by drop casting 10 µL of ink onto the freshly cleaned electrode surfaces. The ink was made by dispersing catalyst powder corresponding to 1.17 µg Pt in 0.5 wt% Nafion in ethanol by ultrasonication (30 min). Home-made single-crystal electrodes Au(111) and Pt(111) as well as monometallic AuNPs and PtNPs from the SAMENS method were measured for comparison to identify voltammetric signals from the target core-shell nanoparticles. Single crystal electrodes were prepared and employed as reported previously.[1] Coiled Pt wire was freshly cleaned by hydrogen flame before use as counter electrode. Freshly made reversible hydrogen electrode (RHE) in the same supporting electrolyte as for measurement was used as a reference electrode (RE) to minimize disturbance from impurities. 5N argon (Ar) was bubbled through the electrolyte solution for 30 min prior to measurement and the electrolyte blanketed with Ar during the measurement to minimize oxygen interference from air. The potential of the RE was calibrated vs. a saturated calomel electrode (SCE) after each measurement and all potentials reported in this work are vs SCE. All glassware including the electrochemical cell were cleaned in boiling 15 vol% HNO_3 followed by rising in Millipore water. The electrochemical surface areas (ECSAs) of Pt and Au on the prepared WEs were determined by integration of the charges in the hydrogen adsorption/desorption (Pt) and metal oxide reduction (Pt and Au) regions of the CVs, Figure S15.

Transmission electron microscopy (TEM) and high-resolution TEM (HR-TEM) were carried out on a Tecnai G2 T20 (200 kV) and Titan Analytical 80 300ST (120 or 300 kV), respectively, from FEI Company (Hillsboro, OR USA). Scanning TEM (STEM) imaging and energy-dispersive X-ray spectroscopy (EDX) mapping were done with HAADF and EDX detectors on the Titan at 300 kV. TEM samples were prepared by dilution or redispersion in Millipore water and deposition of 5 µL on carbon coated copper grids.

The Au@Pt core-shell nanoparticle solution was purified by Amicon filtration to remove excess reactants and any possibly formed small AuNPs or PtNPs. A 100 kDa membrane (Milli-Q, USA) was prepared by soaking in Millipore water for 24 h during which the water was exchanged three times. A buffer solution containing 2.5 mM MES and 1.5 wt‰ starch was used for the

purification to avoid destabilization by removal of MES and starch. 5 mL sample was diluted with 5 mL buffer. The solution was pushed through the membrane by a gentle argon back pressure till 2 mL remained. Two additional filtrations were carried out by filling to 10 mL with buffer in between. Finally, buffer was added to obtain 5 mL retentate used for TEM and EC characterization.
TGA measurements were conducted on a Netzsch STA 409 PC. Around 20 mg of sample were placed in an alumina crucible and heated from r.t. to 1000 °C with a heating rate of 10 °C/min under air flow of 20 mL/min. X-ray photoelectron spectroscopy (XPS) was acquired with a ThermoScientific system at r.t. using Al-Kα radiation (1484.6 eV) as the excitation X-ray source. During analysis pressure was maintained at $2 \cdot 10^{-10}$ mbar. The XPS measurements were then performed in the electron binding energy ranges corresponding to 4f excitations of platinum and gold, and 1s excitations of carbon and oxygen. All samples were measured twice and the reported values are the averages with standard deviations (SD).
The textural properties of the graphitized carbon black supported Au@Pt nanoparticles were determined by nitrogen physisorption analysis using a Micromeritics (Norcross, GA USA) ASAP 2020 with an Automated Gas Adsorption Surface area and Porosimetry Analyzer at liquid nitrogen temperature. The samples were outgassed in vacuum at 200 °C prior to measurement. The surface areas were determined by the Brunauer-Emmett-Teller (BET) method.

Size-controlled synthesis of AuNP seeds

AuNP seeds for size-controlled AuNPs and Au@Pt core-shell NPs were prepared using the SAMENS method (saccharide-based approach to metal nanostructure synthesis)[2] by mixing aqueous $HAuCl_4$ with a buffered solution of glucose and starch. A total volume of 5, 20 or 150 mL were achieved by mixing glucose, starch, buffer (MES or PB at pH 7) and $HAuCl_4$ stock solutions to obtain final concentrations of 10 mM, 0.6 wt%, 10 mM and 2 mM, respectively. Starch, glucose and buffer was mixed first and equilibrated for a few minutes before addition of the gold precursor. Conditions relating to temperature varied slightly depending on the type of shell to be grown and are described in detail in the following sections.
Size-control of AuNPs by the SAMENS method was achieved by sequential addition of reductant (glucose) and stabilizing agent (starch), addition of gold precursor $HAuCl_4$, reaction, extraction of AuNP solution and dilution with water. Initially, a seed solution of AuNPs synthesized in aqueous, MES buffered glucose-starch solution was diluted in water (step 0). The reactant concentrations (not gold) were kept approximately constant and the gold concentration controlled to get a stable and slow increase in the ratio between added precursor and total AuNP surface area. This was calculated with the assumption that the gold precursor was used entirely for the growth of existing spherical particles. The synthesis was carried out in a 100 mL three-necked round-bottomed flask fitted with a condenser with a flow of cooling water and a thermometer. The third neck was used for addition of components and extraction of intermediate size fractions. The temperature was kept at 80 °C with a heating mantle and the solution mixed with a magnetic stirrer. The precursor was added dropwise over a few minutes and reaction was allowed for at least 30 min between each step. Experimental details are given in Table S1. Partitions were taken out after every third step for characterization.

Catalyst preparation

100 mL of standard Au@PtNP solution was prepared and loaded on graphitized carbon black (G-CB) was used as electro- and heterogeneous catalysts. The G-CB was supplied by the Department of Energy Storage and Conversion at DTU and prepared according to their previous report.[3] On the day prior to the catalyst synthesis, 470 mg of the G-CB was dispersed in 100 mL Millipore water, ultrasonicated for 15 min and left with stirring overnight to facilitate good wetting of the support surface and consequently NP dispersion. The support suspension was added to the Au@Pt solution after 1 h of Pt precursor reduction at 95 °C. Heating was terminated after yet 1 h, the suspension was cooled to r.t., and the catalyst isolated by vacuum filtration through a 0.2 µm Nylon membrane. The filter cake was washed with water and EtOH, and dried overnight in air.
Starch around the Pt shell of the Au@Pt/G-CB was removed using a calcination oven (NaberTherm, GmbH). The sample was placed in the oven programmed to reach 300 °C with a heating ramp of 10 °C/min and dwell at this temperature for 1 h. After cooling to r.t., the catalyst was submitted to TGA, XPS, XRD and TEM analysis.
A commercial Pt/G-CB catalyst (20 wt% Pt, <5 nm, 738549, Sigma-Aldrich) was included in the study as reference.

Catalytic hydrogenation

Chemoselective aromatic hydrogenation of BA and BM, and hydrocyclization of LA and MLA was conducted in a 100 mL stainless steel autoclave reactor equipped with an electrically driven mechanical stirrer and an electric heating system (Figure S1). BA, BM, LA, and MLA (0.5 mmol), solvent (50 mL), and catalyst (10 mg for BA & BM, and 50 mg for LA & MLA hydrogenations) were mixed in the autoclave, and the reactor was filled with pure H_2 (AGA, 5.0N) to 5 bar followed by evacuation three times to displace residual air in the reactor. The autoclave was then pressurized with H_2 and heated to the target temperature; BA/BM: 1 bar H_2 at 80 °C, MLA/LA: 20 bar H_2 at 120 °C. The reaction was subsequently initiated by stirring at 320 rpm and maintained for 0.5 to 24 h. The autoclave was allowed to cool to r.t. and aliquots of the reaction mixture was submitted to gas chromatography (GC-FID, Agilent, 6890N) equipped with an HP-5 capillary column (30 m x 0.25 mm, Agilent, J&W) using N_2 as carrier gas. The structure of the product was identified using gas chromatography coupled with mass spectrometry (GC-MS) on an Agilent 6850N spectrometer.

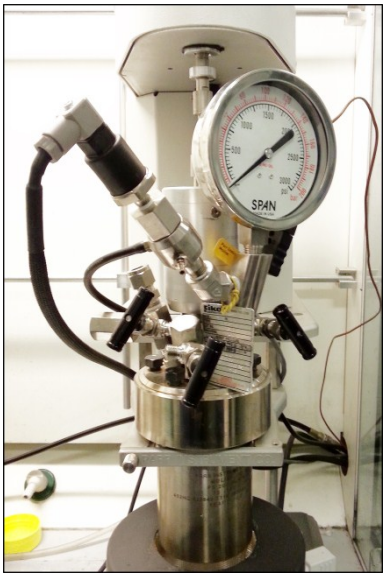

Fig. S1 Experimental setup for catalytic hydrogenation tests.

Supplementary results

Size controlled AuNPs

AuNPs are used as core for the Au@Pt core-shell nanostructures. Controlling the size of AuNPs is an important step in controlling the bimetallic nanostructures. Following the seeded growth method reported by Bastus et al.[4], AuNPs in a range of 8-80 nm were successfully obtained using the SAMENS recipe, Fig. S2 and Table S1.

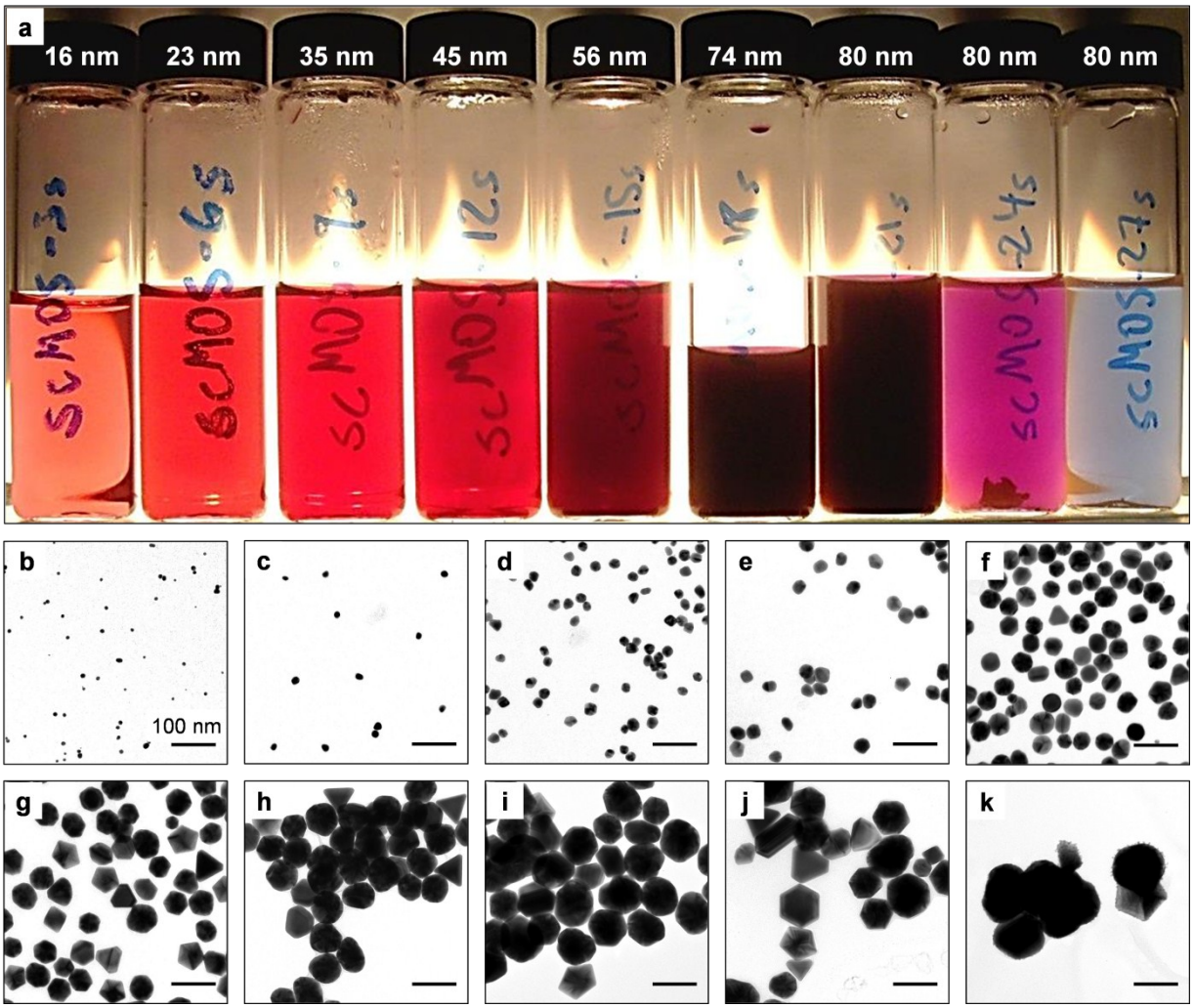

Fig. S2 Fractions of the seeded growth procedure with increasing AuNP size. (a) Photograph of all fractions. The average AuNP size from TEM is indicated on the vial caps. (b-k) TEM images of the AuNP seeds and fractions by increasing size. All images have the same dimensions and the scale bars are 100 nm.

Table S1 Reaction scheme for the size control experiment with added concentrations of reactants. The temperature was kept at 60 °C and stirring maintained throughout the experiment.

Step	MES[a] [mM]	Starch [mM]	Glucose [mM]	$HAuCl_4$ [mM]	Reaction time
0[b]	10.0	0.60	10.0	2.00[c]	28 min
1	7.76	0.47	7.76	0.08	31 min
2	7.74	0.46	7.74	0.15	39 min
3[b]	7.70	0.46	7.70	0.25	31 min
4	8.02	0.48	8.02	0.28	17 min
5	7.97	0.48	7.97	0.42	37 min
6[b]	7.89	0.47	7.89	0.60	33 min
7	8.24	0.49	8.24	0.61	29 min
8	8.14	0.49	8.14	0.84	31 min
9[b]	8.02	0.48	8.02	1.12	23 min
10	8.40	0.50	8.40	1.07	*overnight*
11	8.27	0.50	8.27	1.36	36 min
12[b]	8.12	0.49	8.12	1.70	22 min
13	8.51	0.51	8.51	1.55	30 min
14	8.35	0.50	8.35	1.88	38 min
15[b]	8.18	0.49	8.18	2.26	59 min
16	8.59	0.52	8.59	1.99	86 min
17	8.41	0.50	8.41	2.35	48 min
18[b]	8.23	0.49	8.23	2.74	*overnight*
19	8.64	0.52	8.64	2.38	35 min
20	8.46	0.51	8.46	2.75	26 min
21[b]	8.26	0.50	8.26	3.15	52 min
22	8.67	0.52	8.67	2.69	26 min
23	8.48	0.51	8.48	3.06	87 min
24[b]	8.28	0.50	8.28	3.46	66 min
25	8.69	0.52	8.69	2.91	55 min
26	8.50	0.51	8.50	3.29	35 min
27[b]	8.30	0.50	8.30	3.68	24 min

[a] The MES stock solution was adjusted to pH 7. [b] After reduction of gold precursor at these steps, a fraction was taken out, and the remaining sample diluted with Millipore water and synthesis components. [c] This is the concentration of $HAuCl_4$ in the seed solution. The numbers from step 1 to 27 refer to added precursor and do not include seeds.

In brief, the AuNPs are grown via a sequence of Au precursor reduction, fraction extraction, reactant addition and dilution. 10 fractions of increasing size were obtained and characterized by UV-vis, TEM and NTA, Fig. S3 and Table S2. The localized surface plasmon resonance (LSPR) of AuNPs depends strongly on NP dimensions, thus extinction spectra provide information about size and shape. The $LSPR_{max}$ of the 8 nm spherical starch-capped AuNPs seed solution was just below 520 nm. The AuNP growth causes an increase in the LSPR intensity but no significant shift of the $LSPR_{max}$ at sizes below 40 nm, in agreement with Bastus et al.[4] The band is continuously red-shifted for later fractions to >590 nm. The changes in optical properties is visible by eye and the colloid changes colour from deep red over purple to blue, Fig. S2. All fractions were studied with TEM and NTA to obtain the metal core and hydrodynamic sizes revealing a steady AuNP growth from 8 to 80 nm, Fig. 1b-c and Fig. S3-4.

Table S2 Extinction (UV-vis) and sizing (TEM and NTA) data for the partitions of the size control of AuNPs. Calculated particle size and concentration are based on the initial size of the seed AuNPs (step 0) and an assumption of uniform spherical growth.

Step	UV-vis $LSPR_{max}$ [nm]	Calc. size[a] [nm]	Calc. conc. [#/mL]	TEM Mean ± SD [nm]	NTA Mean ± SD [nm]	NTA Mode ± SD[c] [nm]	NTA Conc. [#/mL]
0	519	8	$7.63 \cdot 10^{13}$	8 ± 2	-	-	-
3	525	15	$1.54 \cdot 10^{12}$	16 ± 2	-	-	-
6	529	22	$1.08 \cdot 10^{12}$	23 ± 3	30 ± 10	27 ± 9	$5.93 \cdot 10^{11}$
9	528	31	$7.54 \cdot 10^{11}$	35 ± 5	50 ± 40	39 ± 4	$1.35 \cdot 10^{12}$
12	528	40	$5.28 \cdot 10^{11}$	45 ± 7	70 ± 60	53 ± 4	$7.51 \cdot 10^{11}$
15	538	49	$3.69 \cdot 10^{11}$	56 ± 6	70 ± 20	62 ± 5	$7.04 \cdot 10^{11}$
18	544	59	$2.59 \cdot 10^{11}$	74 ± 8[b]	70 ± 10	69 ± 8	$7.04 \cdot 10^{11}$
21	555	70	$1.81 \cdot 10^{11}$	80 ± 10[b]	90 ± 30	80 ± 10	$5.64 \cdot 10^{11}$
24	564	81	$1.27 \cdot 10^{11}$	80 ± 10[b]	90 ± 20	90 ± 20	$9.20 \cdot 10^{10}$
27	592	93	$8.87 \cdot 10^{10}$	80 ± 20[b]	110 ± 30	110 ± 20[d]	$5.22 \cdot 10^{10}$

[a] The theoretical size assuming ideal spherical growth of monodisperse particles and gold concentrations as given in Table S1. [b] Highly faceted particles make it difficult to report size by a single number. Aggregation in the final fractions complicates particle sizing further. [c] Since aggregates are counted as large particles with NTA but excluded from the TEM sizing, the mode of the NTA measurement is also provided with SD calculated from the full width half maximum (FWHM) of the distribution (SD = FWHM/2.355). [d] Two maxima of almost equivalent intensity were present and the reported mode is the average of the two.

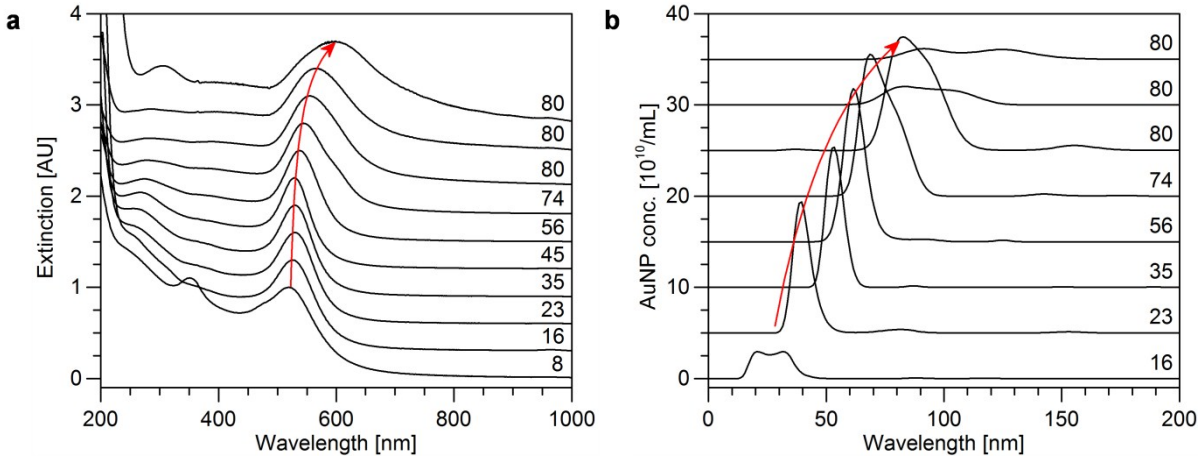

Fig. S3 (a) UV-vis extinction spectra and (b) NTA size distributions of the AuNP seeds and fractions from the seeded growth procedure. Trends are indicated with red arrows and the diameter from TEM given on each curve.

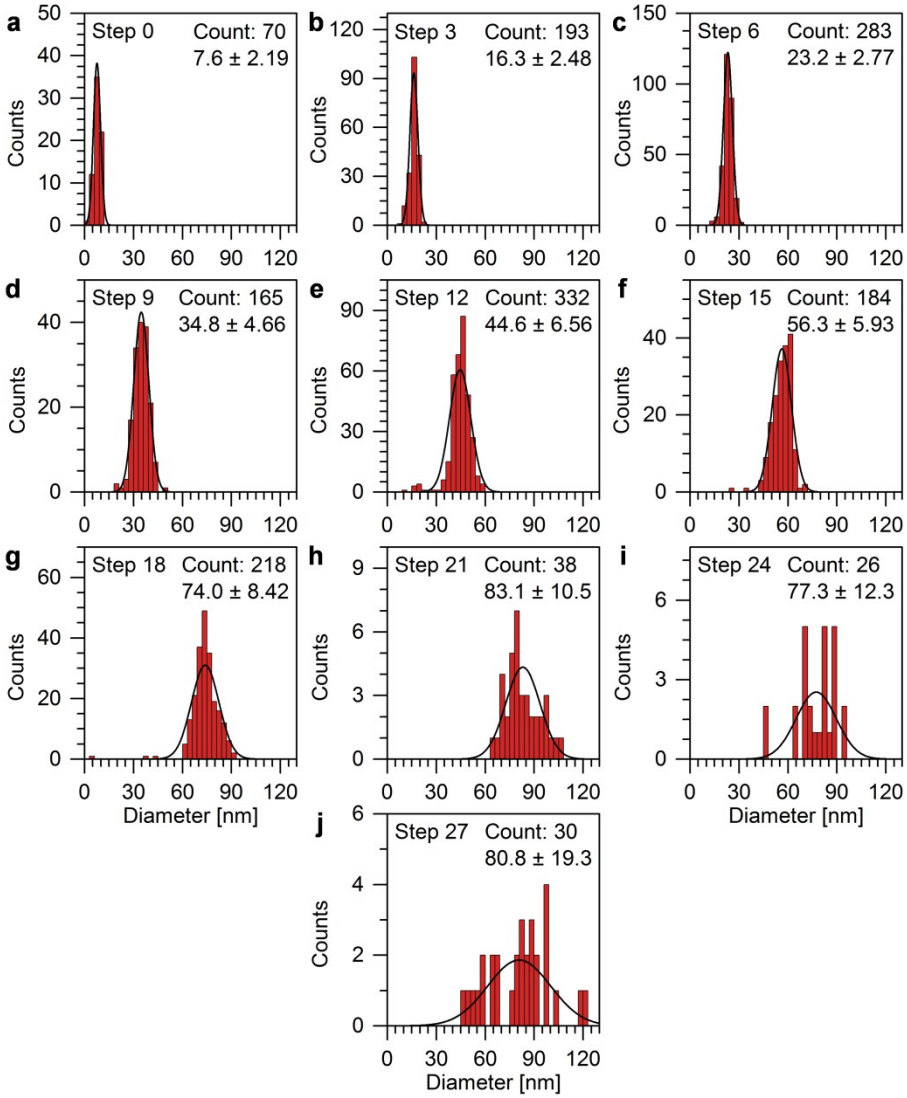

Fig. S4 (a-j) Size distributions of all fractions from the seeded growth procedure for AuNP size control measured from TEM. The number of steps, number of measured particles and the diameter are given in each panel.

Above 50 nm, a significant amount of highly faceted NPs were observed, e.g. flat hexagonal structures and penta-crystalline decahedra, Fig. S2 and S5. As expected for large polycrystalline AuNPs, only low-energy (111) facets are exposed. The colloids of the two last fractions (step 24 and 27) were unstable leading to formation of bulk sediments and a significant decrease in NP concentration. The key to the seeded growth approach is to keep the concentration of reduced precursor (monomer, Au(0)) below the critical nucleation limit in order to avoid nucleation of new NPs.

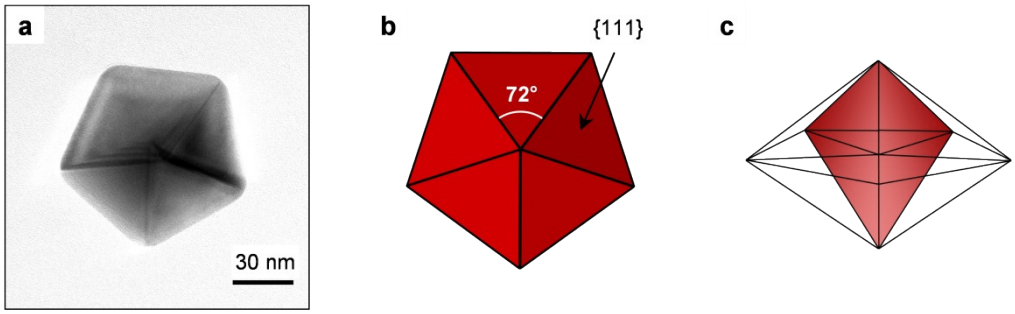

Fig. S5 (a) TEM image and (b-c) model of penta-crystalline Au decahedra.

The aggregation in the final partition led to an overestimation of the NP concentration and thus nucleation of new NPs, Fig. S6. The hydrodynamic size is larger than that observed with TEM as it includes, besides the gold core, the starch coating layer, associated ions and water molecules. Assuming that the starch is neutral, the difference between the size from TEM and NTA is

mainly the starch coating layer which can be estimated to be around 2-4 nm in agreement with previous estimations for starch layers around SAMENS PtNPs.[5]

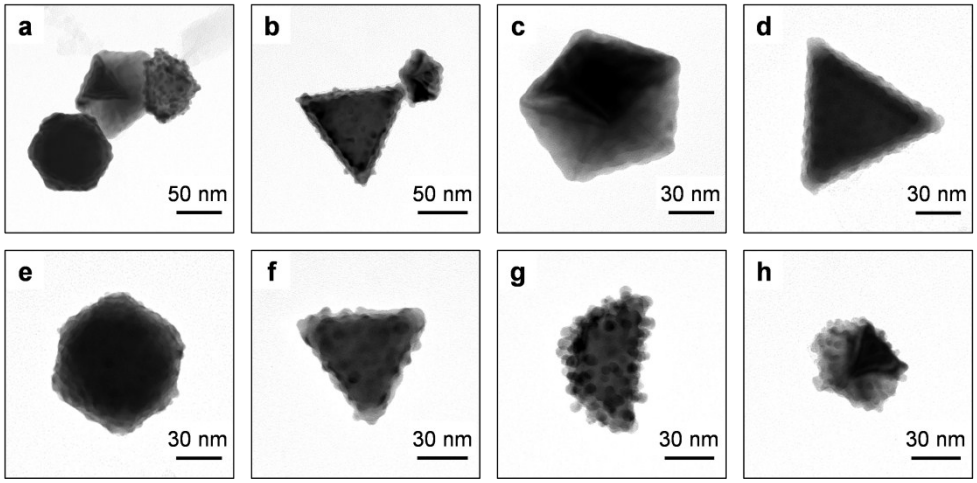

Fig. S6 (a-h) TEM images of large, faceted AuNPs decorated with AuNP seeds found in the last fraction of the seeded growth procedure.

Synthesis of Au-Pt core-shell nanoparticles, Au@Pt NPs

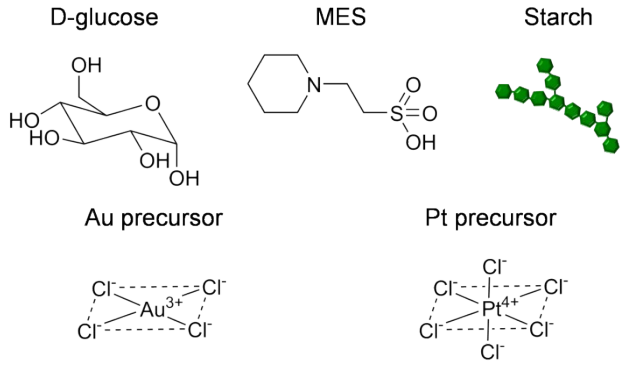

Scheme S1 Molecular structures of glucose, MES, starch, tetrachloroaurate and hexachloroplatinate used for the synthesis of Au@Pt nanostructures.

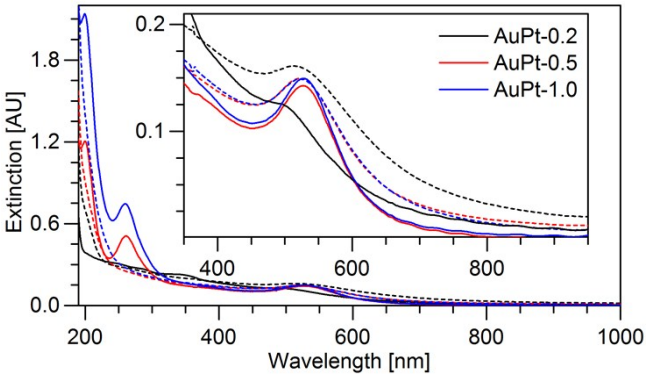

Fig. S7 Extinction spectra of Au@Pt-0.2 (black), -0.5 (red) and -1.0 (blue). Inset shows a closer view of the LSPR peak. Solid lines represent spectra recorded after heating was terminated 1 h after Pt precursor addition and dotted lines spectra recorded 2 years after synthesis.

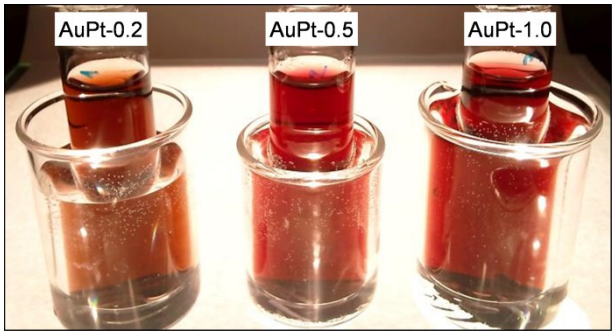

Fig. S8 Photograph of AuPt-0.2, -0.5 and -1.0 showing the brownish colour of the core-shell NPs and the characteristic red colour of the AuNPs.

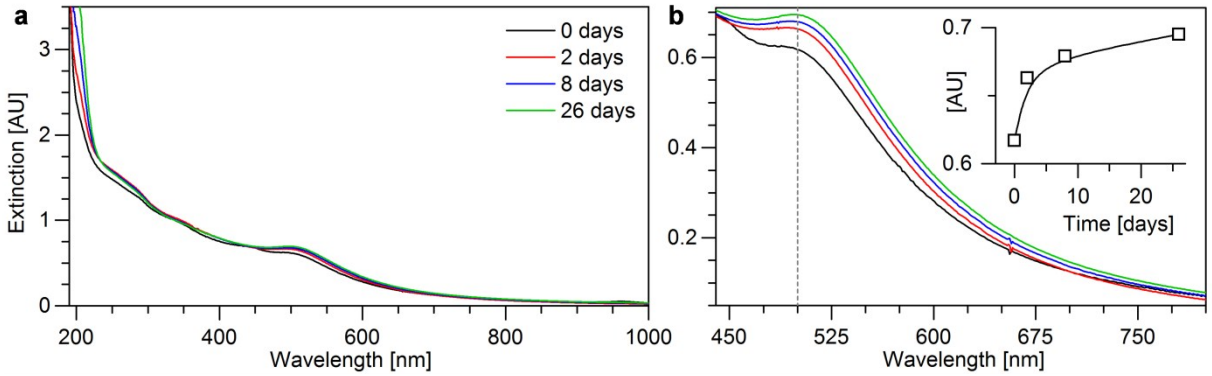

Fig. S9 (a) Extinction spectra of the Au@Pt NPs just after synthesis (black) and after 2, 8 and 26 days. (b) Close view at the changes to the LSPR. Inset shows the extinction at 500 nm over time.

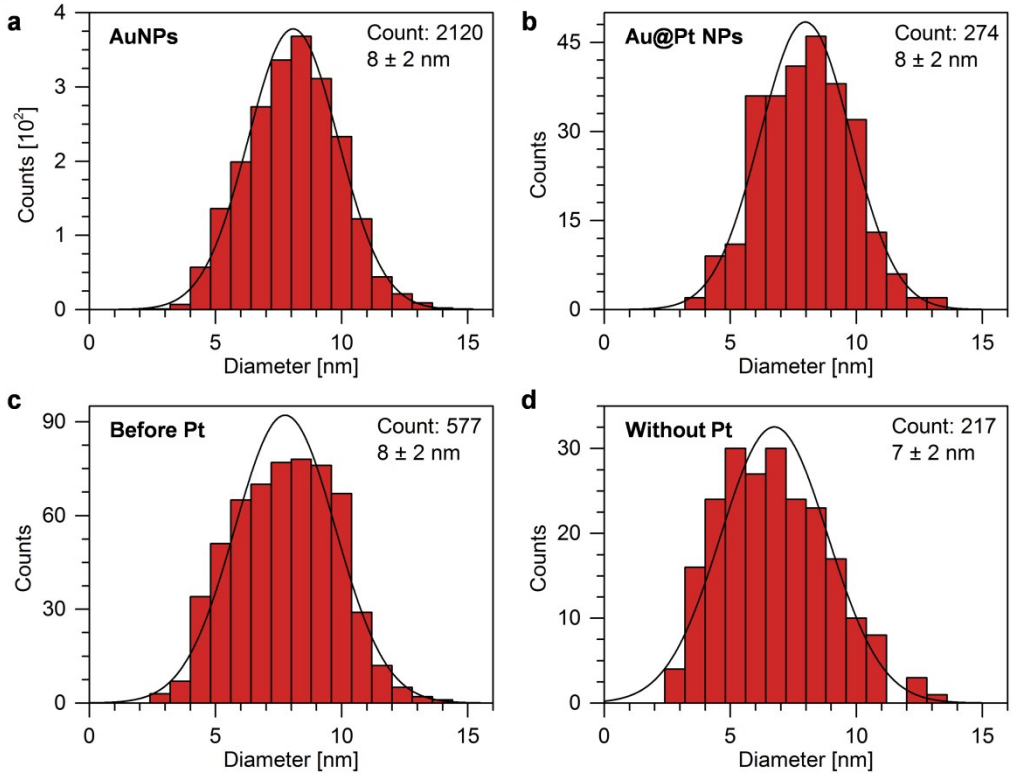

Fig. S10 Size distribution (histogram and Gaussian fit) from TEM measurements of (a) AuNPs, (b) core-shell NPs and AuNPs (c) just before Pt addition and (d) after similar conditions as (b) but without Pt. The number of measured particles and the average size are indicated in each panel.

Table S3 Electrochemical reduction peak potentials of AuO_x and PtO_x in 0.1 M H_2SO_4. All potentials are vs SCE.

Material	AuO_x red.	PtO_x red.
Au@Pt	0.86 V	0.36 V
Au@Pt/G-CB	0.84 V	0.37 V
t-Au@Pt/G-CB	0.84 V	0.37 V
SAMENS PtNP/BPG	-	0.33 V
Pt(111)	-	0.34 V
Pt/G-CB (Sigma)	-	0.38 V
SAMENS AuNP/GC	0.90 V	-
Au(111)	0.83 V	-

Catalyst preparation and catalysis

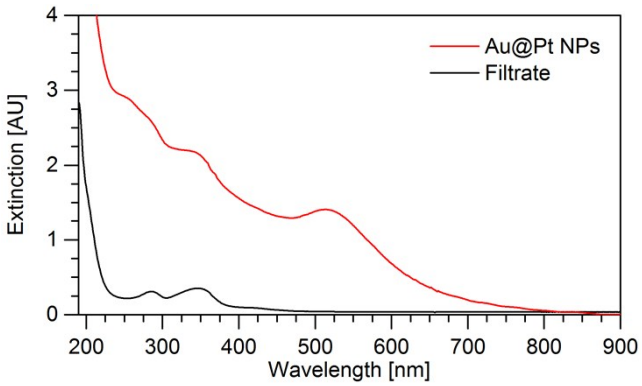

Fig. S11 UV-vis sepctra of as-synthesized Au@Pt NPs before mixing with G-CB (red) and the filtrate obtained after isolation of the prepared Au@Pt/G-CB catalyst (black) showing no evidence of core-shell NPs.

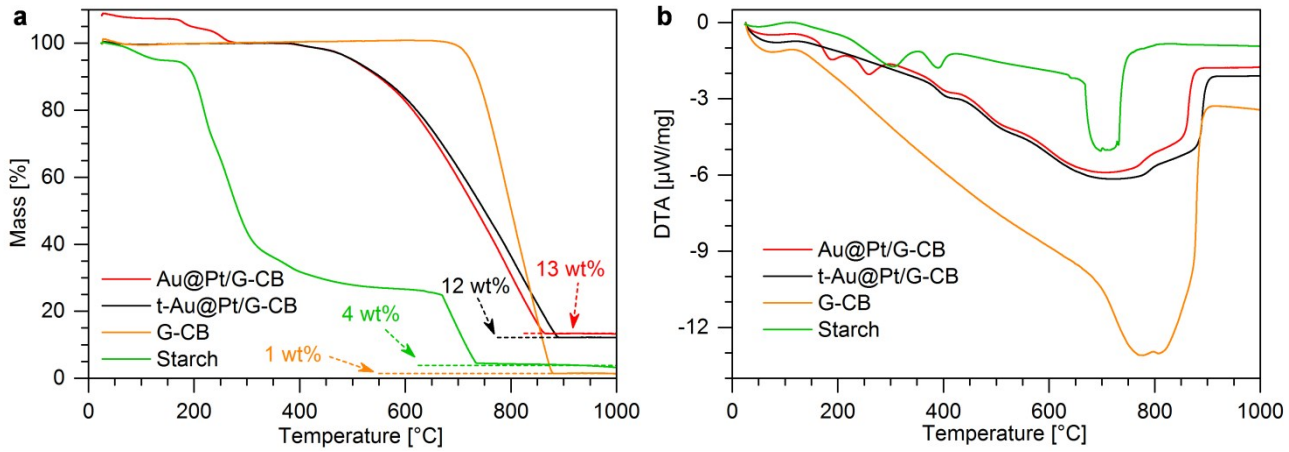

Fig. S12 (a) Thermogravimetric and (b) differential thermal analysis curves for Au@Pt/G-CB before (red) and after (black) thermal treatment to remove starch. Reference curves for pure G-CB support (orange) and starch (green) are also provided.

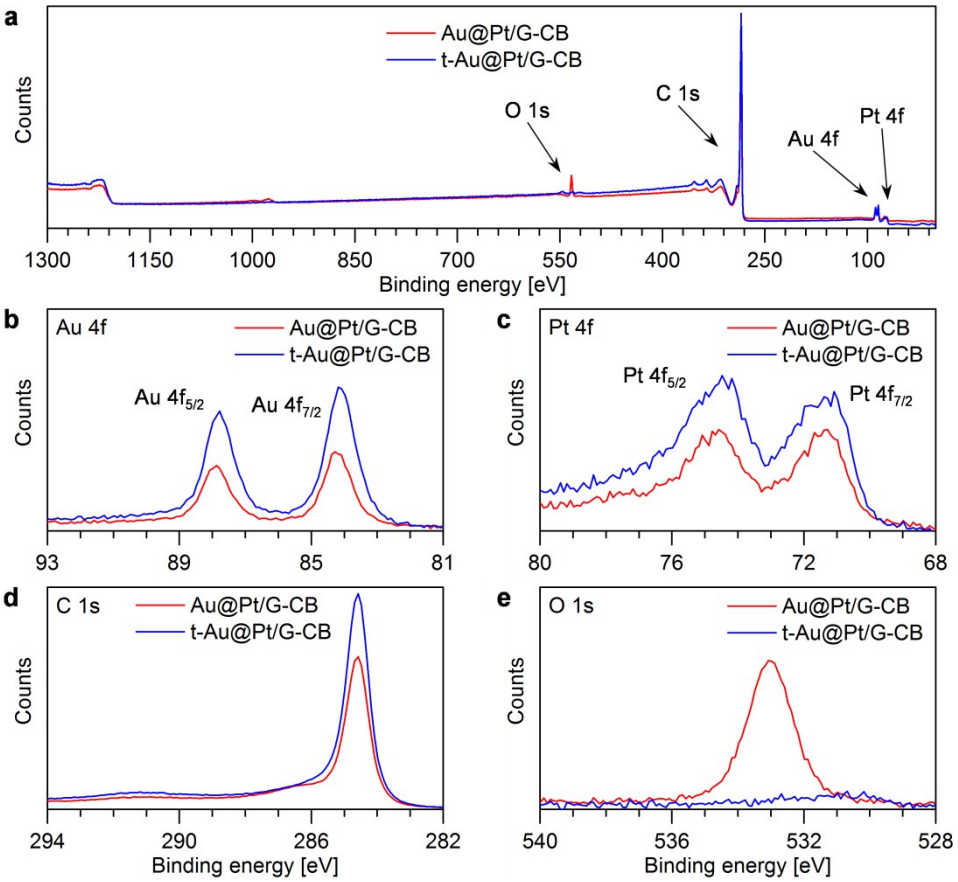

Fig. S13 (a) XPS spectra of Au@Pt/G-CB before (red) and after (blue) thermal treatment. (b-e) Detailed spectra for (b) Au, (c) Pt, (d) C and (e) O.

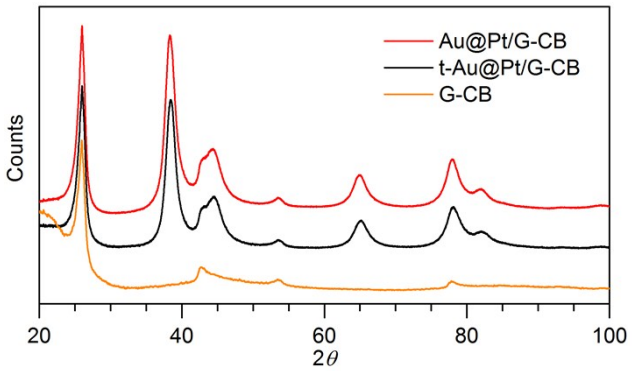

Fig. S14 XRD patterns of Au@Pt/G-CB before (red) and after (black) thermal treatment, and a reference spectrum of pure G-CB (orange). Apart from reflections from the G-CB support, the Au@Pt core-shell catalysts show only reflections from Au/Pt at 38.4, 44.5, 65.1, 78.1 and 82.1°.

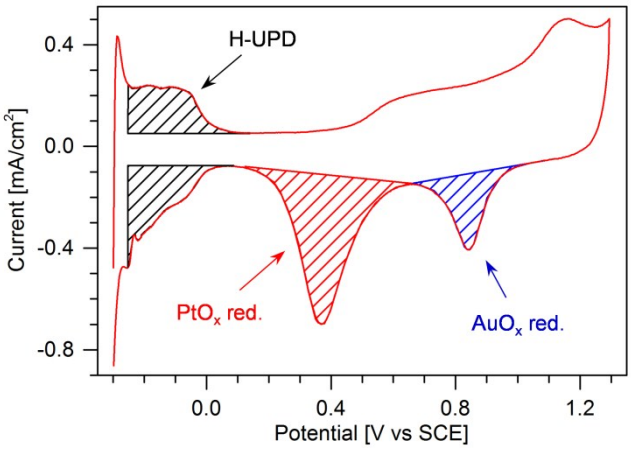

Fig. S15 Electrochemical surface area (ECSA) evaluation based on hydrogen adsorption/desorption (black shaded), or the reduction of Pt (red shaded) or Au (blue shaded) oxides. CV of Au@Pt/G-CB is used as example, also presented in Figure 3.

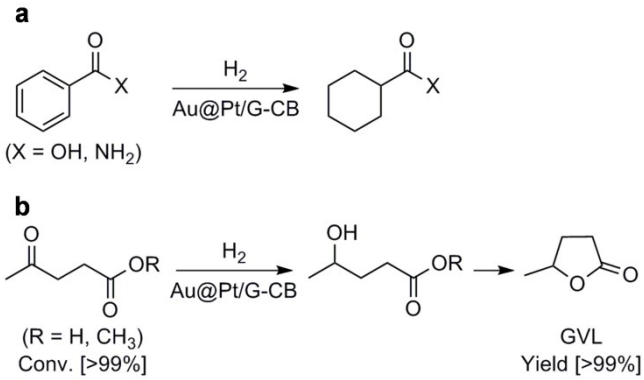

Scheme S2 Reactions catalyzed by Au@Pt NPs. (a) Hydrogenation of the aromatic rings of BA and BM. (b) hydrogenation and cyclization of LA/MLA to form GVL.

Table S4 Benzamide hydrogenation catalyzed by Au@Pt NPs in water or toluene and with or without starch capping.

Condition [a]	I	II	III	IV
Catalyst	Au@Pt/G-CB	Au@Pt/G-CB	t-Au@Pt/G-CB	t-Au@Pt/G-CB
Thermal treatment	No	No	Yes	Yes
Solvent	Water	Toluene	Water	Toluene
Conversion	78%	28%	74%	71%
Selectivity	>99%	>99%	>99%	>99%
TOF [h^{-1}]	10	3.7	9.7	9.3

Reaction conditions: Solvent (50 mL), catalyst (10 mg), benzamide (0.5 mmol), H_2 (1 bar), 80 °C, 24 h, stirring (320 rpm). [a] Labels refer to the conditions presented in Fig. 6.

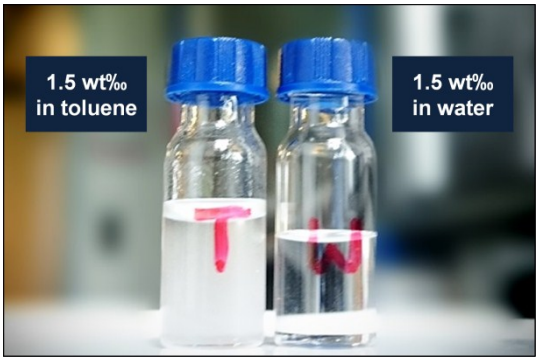

Fig. S16 Photograph of 1.5 wt‰ Zulkowsky starch dissolved in 1 mL toluene (left) and 1 mL water (right). The opaque colour and larger volume of the toluene vial arise from poorly solubilized starch and the presence of solid particles.

Table S5 LA/MLA hydrogenation catalyzed by Au@Pt NPs with or without starch capping, and commercial PtNPs.

Condition [a)]	V	VI	VII	VIII	IX
Catalyst	Au@Pt/G-CB	t-Au@Pt/G-CB	Pt/G-CB	Au@Pt/G-CB	Pt/G-CB
Thermal treatment	No	Yes	No	No	No
Solvent	Water	Water	Water	Water	Water
Reaction time [h]	0.5	0.5	0.5	23	5
Conversion	30%	48%	42%	100%	100%
Selectivity	>99%	>99%	>99%	>99%	>99%
TOF [h^{-1}]	39	62	55	2.7	13

Reaction conditions: Solvent (50 mL), catalyst (1.5 mg Pt), LA/MLA (0.5 mmol), H_2 (20 bar), 120 °C, stirring (320 rpm). [a)] Labels refer to the conditions presented in Scheme 3.

References

1 J. Zhang, Q. Chi, J. Nielsen, E. Friis, J. Andersen and J. Ulstrup, *Langmuir,* 2000, **16,** 7229-7237.

2 C. Engelbrekt, P. S. Jensen, K. H. Sorensen, J. Ulstrup and J. Zhang, *J. Phys. Chem. C,* 2013, **117,** 11818-11828.

3 L. N. Cleemann, F. Buazar, Q. Li, J. O. Jensen, C. Pan, T. Steenberg, S. Dai and N. J. Bjerrum, *Fuel Cells,* 2013, **13,** 822-831.

4 N. G. Bastus, J. Comenge and V. Puntes, *Langmuir,* 2011, **27,** 11098-11105.

5 C. Engelbrekt, K. H. Sorensen, T. Lubcke, J. Zhang, Q. Li, C. Pan, N. J. Bjerrum and J. Ulstrup, *ChemPhysChem,* 2010, **11,** 2844-2853.